

Analysis of heat transfer of hydromagnetic flow over a curved generalized stretching or shrinking surface with convective boundary condition

Muhammad Naveed^{a*}, Zaheer Abbas^b, Qazi Muhammad Zaigham Zia^c

and Muhammad Sajid^d

^aDepartment of Mathematics, Khwaja Fareed University of
Engineering & Information Technology Rahim Yar Khan 62400, Pakistan

^bDepartment of Mathematics, The Islamia University of Bahawalpur,
Bahawalpur 63100, Pakistan

^cDepartment of Mathematics, COMSATS Institute of Information Technology,
Islamabad 46000, Pakistan

^dDepartment of Mathematics and Statistics, International Islamic University,
Islamabad 44000, Pakistan

Abstract: An investigation is carried out to discuss the heat transfer mechanism to an electrically conducting viscous fluid on a curved stretching/shrinking surface incorporated with convective boundary condition. The impact of uniform magnetic field is also considered. The mathematical formulation for the transport of heat and flow phenomena is developed by utilizing a curvilinear coordinates system. The obtained sets of partial differential equations are reconstructed into coupled nonlinear differential equations by incorporating similarity transformations. The numerical solution is attained by employing the shooting method. The obtained solutions are then used to discuss the impacts of various emerging parameters on the temperature and heat transfer across the surface. Dual nature of the solutions are obtained for definite range of convective, suction, magnetic, Prandtl and stretching or shrinking parameters. Comparison of the obtained results with the existing results for a flat sheet is found in acceptable agreement. It is noticed that with an increment in convective parameter increases the temperature of the fluid, while an increase in suction and magnetic parameters decreases the temperature of the fluid for both the solutions.

Keywords: Convective boundary condition, MHD flow, curved stretching/ shrinking sheet viscous fluid, numerical solution.

*Corresponding Author. Tel.: +92 67 3001606

NOMENCLATURE			
B_0	constant magnetic field $[T]$	u	velocity component in the s -direction $[ms^{-1}]$
b	Constant $[-]$	v	velocity component in the r -direction $[ms^{-1}]$
f	dimensionless fluid velocity in r -direction $[ms^{-1}]$	T	Temperature $[K]$
f'	dimensionless fluid velocity in s -direction $[ms^{-1}]$	T_w	surface temperature $[K]$
v_w	mass suction/injection velocity $[ms^{-1}]$	T_∞	ambient fluid temperature $[K]$
k	thermal conductivity of the fluid $[Wm^{-1}K^{-1}]$	T_f	final temperature $[K]$
K	dimensionless radius of curvature $[-]$	Greek symbols	
M	magnetic parameter $[-]$	c_p	specific heat at constant pressure $[Jkg^{-1}K^{-1}]$
p	Pressure $[kgm^{-1}s^{-2}]$	ρ	density of fluid $[kgm^{-3}]$
P	dimensionless pressure $[-]$	μ	dynamic viscosity of the fluid $[m^2s^{-1}]$
Pr	Prandtl number $[-]$	ν	kinematics viscosity of the fluid $[m^2s^{-1}]$
S	Dimensionless mass transfer parameter $[-]$	α	Constant $[-]$
R	radius of curvature $[m]$	γ	Biot number $[=h/k\sqrt{v/a}], [-]$
Re_s	local Reynold number $[-]$	θ	dimensionless fluid temperature $\theta(\eta) = [T - T_\infty / T_f - T_\infty] [-]$
s	flow directional coordinate along the stretching surface $[m]$	σ	electrical conductivity $[sm^{-1}]$
r	distance normal to stretching surface $[m]$		

1. Introduction

The analysis of heat transfer mechanism on a stretching or shrinking sheet is a significant field of research from last few decades. The boundary layer flow towards a stretching sheet have abundant practical applications including glass blowing, paper production, metal spinning, extrusion of plastic sheets and many more. The finishing of the ultimate product in these applications has a strong dependence on the amount of heat transfer across the surface and the fluid. This fact is explained by Karwe and Jaluria [1]. The heat transfer analysis in fluid flow by considering a constant surface temperature is rich and well established area of research and for more information readers are pointed to the book by Incropera [2].

Crane [3] examined the boundary layer flow towards a stretching sheet and obtained an exact solution. Miklavcic and Wang [4] discussed for the first time the boundary layer flow of a viscous fluid on a shrinking wall. They also pointed out the existence and (non) singularity of both numerical and closed form solutions. Bhattacharyya [5] analyzed the effects MHD flow and heat transfer subjected to heat source or sink towards a shrinking wall with mass suction. Bejan [6] examined a similarity solution by taking the boundary condition of invariable heat flux at the surface. Aziz [7] studied the classical problem of thermal boundary layers and hydrodynamic flow towards a flat plate incorporated with convective surface boundary condition. The research work to study flow and heat transfer mechanism for different kind of flow geometries are discussed by many authors, the interesting readers see the articles [8-20] and references therein.

The application of an applied magnetic field to the flow has extensive application in cosmic fluid dynamics, polymer industry, metallurgy, geophysics and in the motion of earth's core. Jafar et al. [21] discussed the hydromagnetic flow and heat transfer towards stretching/shrinking sheet in with viscous dissipation and Joule effects. Kameswaran et al. [22] examined the impacts of hydromagnetic nanofluid flow caused by stretching/shrinking surface with chemical reaction and viscous dissipation effects. Rosca [23] examined the MHD flow past a permeable shrinking surface. Numerical solution of hydromagnetic flow with impacts of viscous dissipation was studied by Mishra and Jena [24]. For more detail regarding the flow phenomenon with magnetic field the readers are directed to the articles [25-31].

Generally, the flow problem on a stretching surface have been considered towards a flat plate. However, Sajid et al. [32] has given a unique concept of research by considering a curved stretching sheet having an invariable curvature and employed a curvilinear coordinate system to formulate the flow equations. The impacts of heat transfer on a MHD flow over a curved stretching surface was examined by Abbas et al. [33]. Naveed et al. [34] explored the hydromagnetic micropolar fluid flow due to a curved stretching sheet with thermal radiation. Recently, Abbas et al. [35] studied the influence of thermal radiation on MHD slip flow of a nanofluid towards a curved stretching surface.

The prime intention of this study is to extend the investigation carried out by Aziz [7] for convective boundary condition to the flow towards a curved generalized stretching/shrinking

surface by considering constant magnetic field. The dual solution occurs for the present flow problem in case of curved shrinking surface. The formulation of the problem is given in section 2. Section 3 consists of discussion of the obtained numerical results. Some conclusions are summarized in section 4.

2. Formulation

Consider the steady, incompressible boundary layer flow of a viscous fluid on a curved stretching or shrinking sheet curled in a circle of radius R with mass transfer in a static fluid. It is considered that the sheet is being stretched or shrunk in s -direction with a velocity $u_w = bs$, where $b > 0$ indicates the stretching and $b < 0$ indicates the shrinking of the sheet. Furthermore, it is also considered that v_w is the constant mass transfer velocity in the fluid with $v_w > 0$ for suction and $v_w < 0$ for injection. A uniform magnetic field of strength B_0 is applied in the r -direction. The impacts of induced magnetic field can be neglected by considering the low magnetic Reynolds number regime. The surface temperature of the sheet is maintained at constant value of T_w by using convective heat transfer condition and the temperature of the ambient fluid is T_∞ . The boundary layer equations that governs the current flow situation are

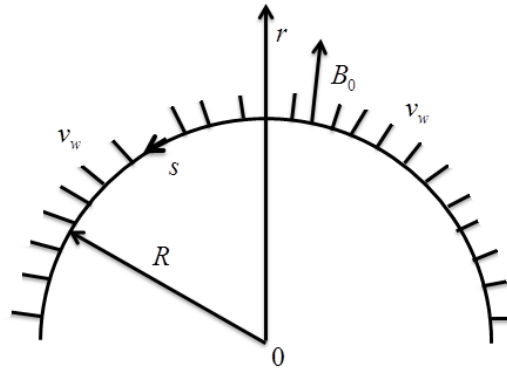


Fig. 1 Geometry of the flow problem

$$\frac{\partial}{\partial r} \{ (r+R)v \} + R \frac{\partial u}{\partial s} = 0, \quad (1)$$

$$\frac{u^2}{r+R} = \frac{1}{\rho} \frac{\partial p}{\partial r}, \quad (2)$$

$$v \frac{\partial u}{\partial r} + \frac{Ru}{r+R} \frac{\partial u}{\partial s} + \frac{uv}{r+R} = -\frac{1}{\rho} \frac{R}{r+R} \frac{\partial p}{\partial s} + \left(\frac{\partial^2 u}{\partial r^2} + \frac{1}{r+R} \frac{\partial u}{\partial r} - \frac{u}{(r+R)^2} \right) - \frac{\sigma B_0^2}{\rho} u, \quad (3)$$

$$\rho c_p \left[v \frac{\partial T}{\partial r} + \frac{Ru}{r+R} \frac{\partial T}{\partial s} \right] = k \left(\frac{\partial^2 T}{\partial r^2} + \frac{1}{r+R} \frac{\partial T}{\partial r} \right), \quad (4)$$

where v and u indicates the velocity components in r and s -directions, respectively, and k, ν, σ, p, ρ and T represents the thermal conductivity, kinematic viscosity, electrical conductivity, pressure, density, and temperature of the fluid respectively. Viscous dissipation in the energy equation is also neglected in the present study.

The boundary conditions for the current study are

$$\begin{aligned} u = -bs, \quad v = -v_w, \quad -k \frac{\partial T}{\partial r} = h_f (T_f - T_w) \quad \text{at } r = 0, \\ u \rightarrow 0, \quad \frac{\partial u}{\partial r} \rightarrow 0, \quad T \rightarrow T_\infty \quad \text{as } r \rightarrow \infty, \end{aligned} \quad (5)$$

In above equation h_f denotes the convective heat transfer coefficient, b is constant having dimension (time)⁻¹ and T_f is the final temperature of the fluid with $T_f > T_w > T_\infty$.

Our interest lies in reducing the problem given in equations (1)-(5) into differential equations. For this purpose we incorporate the similarity variables of the form

$$\begin{aligned} u = asf'(\eta), \quad v = \frac{-R}{r+R} \sqrt{av} f(\eta), \quad p = \rho a^2 s^2 P(\eta), \\ \eta = \sqrt{\frac{a}{\nu}} r, \quad \theta(\eta) = \frac{T - T_\infty}{T_f - T_\infty}. \end{aligned} \quad (6)$$

The transformed equations in new variables are

$$\frac{\partial P}{\partial \eta} = \frac{f'^2}{\eta + K}, \quad (7)$$

$$\begin{aligned} \frac{2K}{\eta + K} P = f''' + \frac{f''}{\eta + K} - \frac{f'}{(\eta + K)^2} - \frac{K}{\eta + K} f'^2 \\ + \frac{K}{\eta + K} ff'' + \frac{K}{(\eta + K)^2} ff' - Mf', \end{aligned} \quad (8)$$

$$\theta'' + \frac{\theta'}{\eta + K} + \frac{\text{Pr} K}{\eta + K} f \theta' = 0, \quad (9)$$

$$\begin{aligned} f(0) = S, \quad f'(0) = b/a = \alpha, \quad \theta'(0) = -\gamma(1 - \theta(0)), \\ f'(\infty) = 0, \quad f''(\infty) = 0, \quad \theta(\infty) = 0, \end{aligned} \quad (10)$$

where $S = v_w / \sqrt{av}$ is the mass transfer parameter such that $S > 0$ indicates suction and $S < 0$ is for injection and α represents the stretching/shrinking parameter with $\alpha > 0$ for the stretching parameter and $\alpha < 0$ for the shrinking parameter. Also

$M = \sigma B_0^2 / a \rho$, $Pr = \mu c_p / k$, $K = R\sqrt{a/\nu}$ and $\gamma = h/k\sqrt{\nu/a}$, is the magnetic parameter, Prandtl number, dimensionless radius of curvature and Biot number respectively.

Elimination of pressure between equations (7) and (8) yield

$$\begin{aligned} f^{iv} + \frac{2f'''}{\eta+K} - \frac{f''}{(\eta+K)^2} + \frac{f'}{(\eta+K)^3} - \frac{K}{\eta+K}(ff'' - ff''') \\ - \frac{K}{(\eta+K)^2}(f'^2 - ff'') - \frac{K}{(\eta+K)^3}ff' - Mf'' - M\frac{f'}{\eta+K} = 0, \end{aligned} \quad (11)$$

After obtaining the velocity profile $f(\eta)$, the pressure could be obtained from Eq. (8) as

$$P(\eta) = \frac{\eta+K}{2K} \left[\begin{aligned} &f''' + \frac{f''}{\eta+K} - \frac{f'}{(\eta+K)^2} - \frac{K}{\eta+K}f'^2 \\ &+ \frac{K}{\eta+K}ff'' + \frac{K}{(\eta+K)^2}ff' - Mf' \end{aligned} \right]. \quad (12)$$

Physically the quantities of interest are the wall temperature, local Nusselt number and the skin friction coefficient at the surface, which are defined as

$$-k \frac{\partial T}{\partial r} = h_f (T_f - T_w), N_{u_s} = \frac{sq_w}{k(T_w - T_\infty)}, C_f = \frac{\tau_{rs}}{\rho u_w^2}, \quad (13)$$

where q_w and τ_{rs} are the heat flux and shear stress at the wall along the s -direction which is given by

$$q_w = -k \frac{\partial T}{\partial r} \Big|_{r=0}, \quad \tau_{rs} = \mu \left(\frac{\partial u}{\partial r} - \frac{u}{(r+R)} \right) \Big|_{r=0}. \quad (14)$$

Using Eq. (6), (14) with the help of Eq. (13) becomes

$$\begin{aligned} Re_s^{1/2} C_f &= f''(0) - \frac{f'(0)}{K}, \\ \theta(0) &= 1 - \frac{\theta'(0)}{\gamma}, \\ Re_s^{-1/2} N_{u_s} &= -\theta'(0). \end{aligned}$$

where $Re_s = as^2/\nu$ represents the local Reynolds number.

3. Result and discussions

Numerical solutions of the nonlinear boundary value problem composed of equation (9) and (11) subject to boundary conditions (10) are attained in terms of temperature and fluid velocity by using the shooting method with Runge-Kutta algorithm. The dual solutions in case of shrinking flow are attained by employing different initials values for $f''(0)$, $f'''(0)$ and $\theta'(0)$,

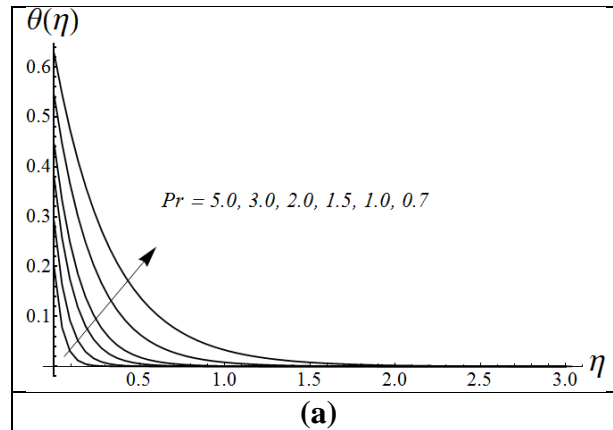
where entire velocity and temperature fields fulfill the free stream boundary conditions asymptotically for entire values of the fluid parameters and choosing a suitable finite value of η_∞ (where η_∞ corresponds to $\eta \rightarrow \infty$). The impacts of radius of curvature on pressure distribution has already been explained in Abbas et al. [33]. The impacts of some physical parameters of interest on the fluid velocity and temperature field are plotted and given in Figs. 2-9. Tables 1-3 are made to give the comparison of current results with the available results in the literature [7, 19, 36, 37] as a special case of flat stretching or shrinking sheet.

Fig. 2 shows the variation in the temperature field $\theta(\eta)$ for several values of the Prandtl number Pr in the case of stretching sheet ($\alpha = 2$) with $S = 4, -4$ respectively. From Fig. 2(a) it can be seen that both the temperature and also the thermal boundary layer thickness is decreased with raise in the parameter Pr in the case of suction $S = 4$. For the case of injection $S = -4$, it is found from Fig. 2(b) that the thermal boundary layer is blown away from the sheet and heat flux at the surface becomes very small. Further, it is noticed that the thermal boundary layer thickness is still thinner for higher values of Pr , but the temperature distribution is quite interesting. Fig. 3 depicts the dual solutions of the temperature field $\theta(\eta)$ for different values of the Prandtl number Pr when ($\alpha = -2$) with $S = 4, \gamma = 5, \lambda = 0.2$ and $K = 10$. It can be seen from this Fig. that for both solutions the temperature of fluid and the thermal boundary layer thickness decrease with raise Pr . Fig.4 elucidates the dual solutions of the temperature distribution $\theta(\eta)$ for different values of the mass suction parameter S in the case of shrinking flow ($\alpha = -1.5$) by keeping other parameters fixed. From this Fig. it is evident that both the temperature and thermal boundary layer thickness decrease by increasing the mass suction parameter S . The influence of the mass suction/injection parameter S on the temperature profile $\theta(\eta)$ is shown in Fig. 5, for stretching flow ($\alpha = 2$) with $Pr = 0.7, \gamma = 2, \lambda = 0.2$ and $K = 10$. It is noticed from this Fig. that the rate of heat transfer to the fluid is decreased with an increase in mass suction/injection parameter S i.e. S changes from -2 to 2 . Fig. 6 illustrates the impacts of the convective parameter (or Biot number) γ on the temperature distribution $\theta(\eta)$ for shrinking flow ($\alpha = -2$). It is observed from this Fig. that for both solutions the temperature of fluid decreases with an increase in convective parameter γ . Fig. 7 presents the dual solutions of temperature field $\theta(\eta)$ for divers values of

the magnetic parameter M in case of shrinking flow ($\alpha = -1.5$) with other fluid parameters are fixed.. It can be seen that the temperature and the thermal boundary layer thickness decreases with raise in magnetic parameter M .

Fig. 8 is plotted to show the variation of $\theta'(0)$ with the suction parameter S for divers values of the magnetic parameter M . It is clear from this Fig. that for $M = 0.2$, dual solution exists for $S_c < S = 3.092451$ (where S_c is the critical value of S) and no solution exists for $S < S_c$. For $M = 0.19$, the duality of solution is obtained for $S \geq S_c$, and no dual solution is found for $S < S_c$. The dual nature of solution for $M = 0.18$ is obtained for $S \geq S_c = 3.301900$ and the solution vanishes for $S < S_c = 3.301900$. Fig. 9 is plotted to present the variation of $\theta'(0)$ with the suction parameter S for various values of the Prandtl number Pr . It can be seen from this Fig. that dual solutions exist for $S \geq S_c = 3.092451$, for different values of the Prandtl number while no dual solution exists for $S < S_c = 3.092451$..

Table 1 indicates the numerical values of the local Nusselt number $-\theta'(0)$ for several values of Pr when $\alpha = 1, S = M = 0$ and $\gamma = 1000$ in the case of flat stretching sheet ($K \rightarrow \infty$). From this table, the comparison of the present results with those reported by Makinde and Aziz [17], Wang [37] and Khan and Pop [36] and is given and found in good agreement. Tables 2 and 3 shows the absolute values of surface temperature $\theta(0)$ and Nusselt number $-\theta'(0)$, when $M = S = 0$, for diverse values of Pr and γ in case of flat stretching sheet (taking $K \rightarrow \infty$). It is worth mentioning from this table that the present numerical results are in acceptable agreement with the result reported by Aziz [7].



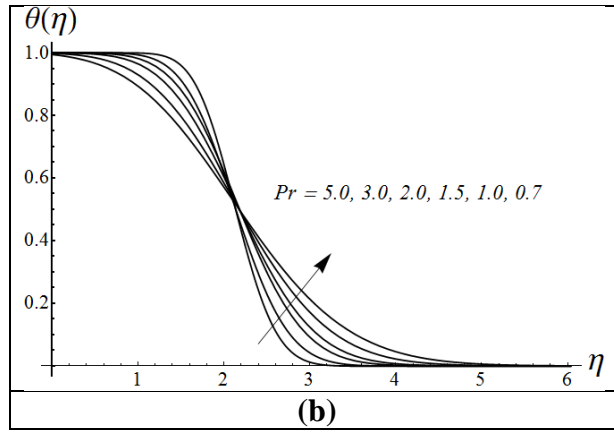


Fig. 2: Variation of Pr on $\theta(\eta)$ under suction $S=4$ (a) and injection $S=-4$ (b) with $\alpha=2, \gamma=5, K=10$ and $M=0.2$ fixed.

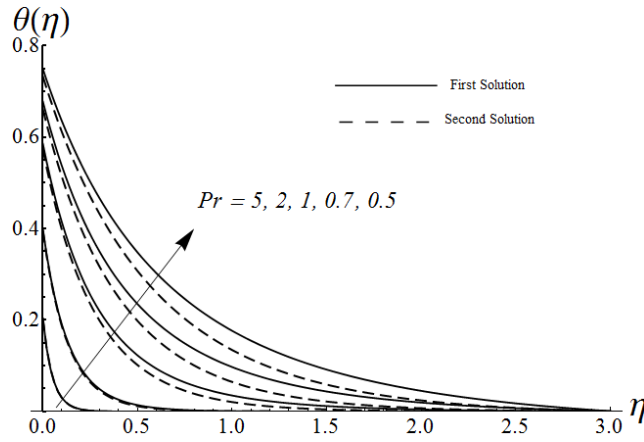


Fig. 3: Variation of Pr on the $\theta(\eta)$ with $\alpha=-2, \gamma=5, S=4, K=10$ and $M=0.2$ fixed.

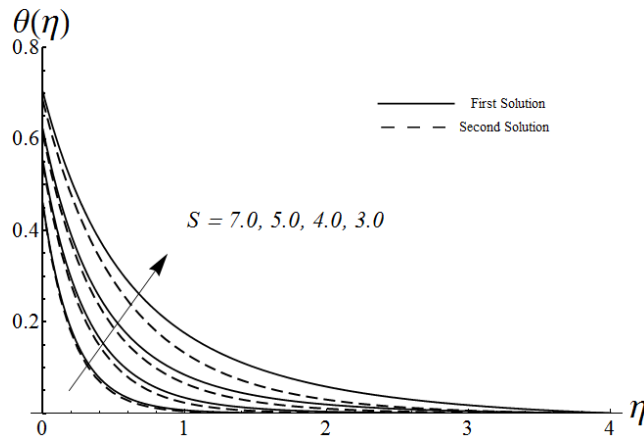


Fig. 4: Variation of S on $\theta(\eta)$ with $\alpha=-1.5, \gamma=4, Pr=0.7, K=10$ and $M=0.2$ fixed.

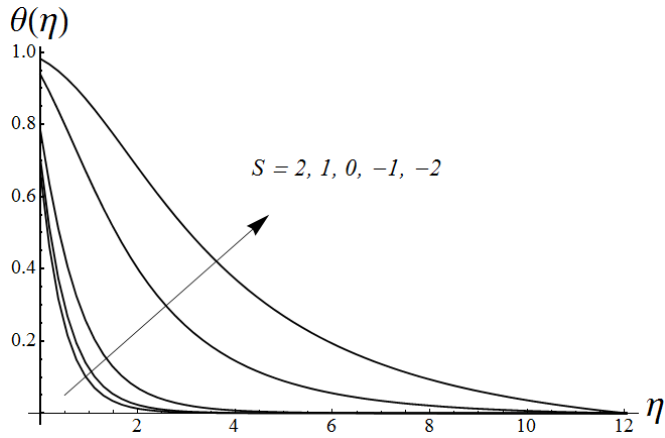


Fig. 5: Variation of S on the temperature distribution $\theta(\eta)$ with $\alpha = 2, \gamma = 4, Pr = 0.7, K = 10$ and $M = 0.2$ fixed.

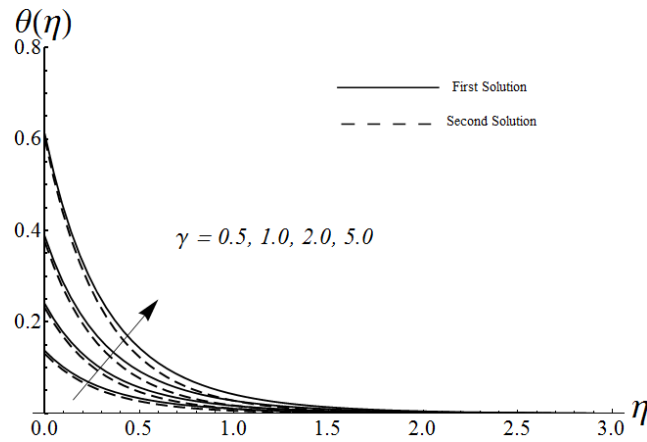


Fig. 6: Variation of γ on $\theta(\eta)$ with $\alpha = -2, S = 5, Pr = 0.7, K = 10$ and $M = 0.2$ fixed.

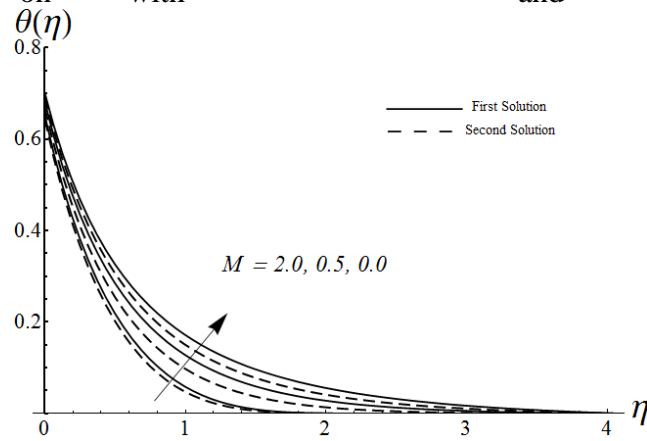


Fig. 7: Variation of M on $\theta(\eta)$ with $\alpha = -1.5, \gamma = 4, Pr = 0.7, K = 10$ and $S = 3$ fixed.

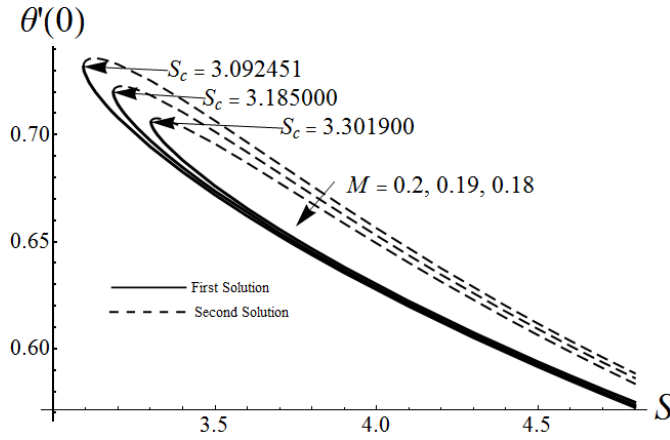


Fig. 8: Variation of M on $Re_s^{-1/2} Nu_s$ with S by keeping $\alpha = -1.5, Pr = 0.7, K = 10$ and $\gamma = 4$ fixed.

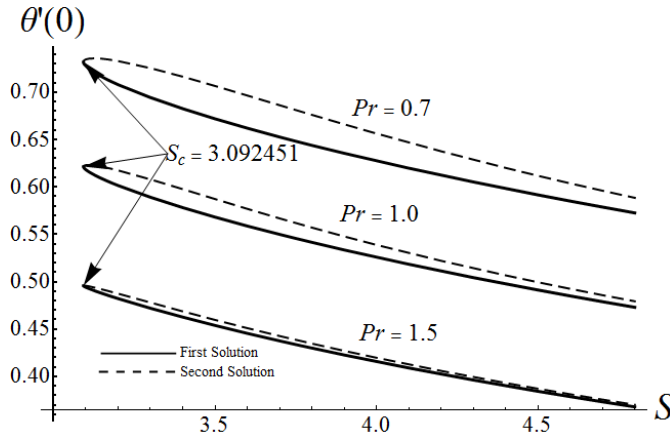


Fig. 9: Variation of Pr on $Re_s^{-1/2} Nu_s$ with S by keeping $\alpha = -1.5, M = 0.2, K = 10$ and $\gamma = 4$ fixed.

Table 1: Numerical values of $-\theta'(0)$ for various values of Pr by keeping $\alpha = 1, S = M = 0, \gamma = 1000$ and $K = 1000$.

Pr	Khan and Pop [36]	Wang [37]	Makinde and Aziz [17]	Present results
0.07	0.0663	0.0656	0.0656	0.0656
0.20	0.1691	0.1691	0.1691	0.1691
0.70	0.4539	0.4539	0.4539	0.4539
2.00	0.9113	0.9114	0.9114	0.9114
7.00	1.8954	1.8954	1.8954	1.8954
20.0	3.3539	3.3539	3.3539	3.3539
70.0	6.4621	6.4622	6.4622	6.4622

Table 2: Numerical values of $-\theta'(0)$ for various values of γ and Pr by keeping $K = 1000$.

γ	Pr = 0.1		Pr = 0.72		Pr = 10	
	Aziz [7]	Present results	Aziz [7]	Present results	Aziz [7]	Present results
0.05	0.0373	0.0373	0.0428	0.0428	0.0468	0.0468
0.10	0.0594	0.0594	0.0747	0.0747	0.0879	0.0879
0.20	0.848	0.848	0.1193	0.1193	0.1569	0.1569
0.40	0.1076	0.1076	0.1700	0.1700	0.2582	0.2582
0.60	0.1182	0.1182	0.1981	0.1981	0.3289	0.3289
0.80	0.1243	0.1243	0.2159	0.2159	0.3812	0.3812
1.0	0.1283	0.1283	0.2282	0.2282	0.4213	0.4213
5.0	0.1430	0.1430	0.2791	0.2791	0.6356	0.6356
10.0	0.1450	0.1450	0.2871	0.2871	0.6787	0.6787
20.0	0.1461	0.1461	0.2913	0.2913	0.7026	0.7026

Table 3: Numerical values of the surface temperature $\theta(0)$ for different values of γ and Pr by keeping $K = 1000$.

γ	Pr = 0.1		Pr = 0.72		Pr = 10	
	Aziz [7]	Present results	Aziz [7]	Present results	Aziz [7]	Present results
0.05	0.2536	0.2536	0.1447	0.1447	0.0643	0.0643
0.10	0.4046	0.4046	0.2528	0.2528	0.1208	0.1208
0.20	0.5761	0.5761	0.4035	0.4035	0.2155	0.2155
0.40	0.7310	0.7310	0.5751	0.5751	0.3546	0.3546
0.60	0.8030	0.8030	0.6699	0.6699	0.4518	0.4518
0.80	0.8446	0.8446	0.7302	0.7302	0.5235	0.5235
1.0	0.8717	0.8717	0.7718	0.7718	0.5787	0.5787
5.0	0.9714	0.9714	0.9441	0.9441	0.8729	0.8729
10.0	0.9855	0.9855	0.9713	0.9713	0.9321	0.9321

20.0	0.9927	0.9927	0.9854	0.9854	0.9649	0.9649
------	--------	--------	--------	--------	--------	--------

4. Concluding remarks

The boundary layer flow and heat transfer in a viscous fluid over a curved generalized stretching or shrinking sheet with convective boundary condition is carried out. This study is more general and novel by considering convective heating boundary condition instead of a constant heat flux or a constant temperature of the wall. The transformed similarity equations are solved numerically and the influence of various pertinent parameters on the temperature distribution is analyzed, presented and discussed graphically. Dual solutions occur for shrinking flow for certain values of generalized shrinking parameter α . An increment in the surface convective parameter γ yields to increase in the temperature of the fluid which results in an increase in the heat transfer rate. The enhancement in the magnetic parameter M leads to decrease the temperature of the fluid.

Acknowledgment: We are thankful to the reviewers for their encouraging comments and constructive suggestions to improve the quality of the manuscript.

References

- [1] Karwe, M. V. and Jaluria, Y., Numerical solution of thermal transport associated with a continuous moving flat sheet in materials processing, *J. Heat Transf.* 113 (1991), pp. 612-619.
- [2] Incropera, F. P., Fundamental of heat and mass transfer, 6th ed. John Wiley and Son, New York. (2007).
- [3] Crane, L. J., Flow past a stretching plate, *Zeits. Ange. Mathe. Phys. (ZAMP)*. 21 (1970), pp. 645-647.
- [4] Miklavcic, M. and Wang, C. Y., Viscous flow due to a shrinking sheet, *Quar. Appl. Mathe.* 64 (2006), pp. 283-290.
- [5] Bhattacharya, K., Effect of heat source/sink on MHD flow and heat transfer over a shrinking sheet with mass suction, *Chem. Eng. Res. Bul.* 15 (2011), pp. 12-17.
- [6] Bejan, A., Convective Heat Transfer, 3rd ed. John Wiley and Son, New York. pp. 51-54 (2004).
- [7] Aziz, A., A similarity solution for laminar thermal boundary layer over a flat plate with a convective surface boundary condition, *Commun. Nonlinear Sci. Numer. Simul.* 14 (2009), pp. 1064-1068.
- [8] Ishak, A., Similarity solutions for flow and heat transfer over a permeable surface with convective boundary condition, *Appl. Math. Compu.* 217 (2010), pp. 837-842.
- [9] Sheikholeslami, M., Darzi, M. and Sadoughi, M., Heat transfer improvement and pressure drop during condensation of refrigerant-based nanofluid; an experimental procedure, *Int. J. Heat Mass Transf.* 122 (2018), pp. 643-650.
- [10] Sheikholeslami, M. and Shehzad, S. A., Simulation of water based nanofluid convective flow inside a porous enclosure via non-equilibrium model, *Int. J. Heat Mass Transf.* 120 (2018), pp. 1200-1212.

- [11] Sheikholeslami, M. and Seyednezhad, M., Simulation of nanofluid flow and natural convection in a porous media under the influence of electric field using CVFEM, *Int. J. Heat Mass Transf.* 120 (2018), pp. 772-781.
- [12] Sheikholeslami, M., Numerical investigation of nanofluid free convection under the influence of electric field in a porous enclosure, *J. Molec. Liq.* 249 (2018), pp. 1212-1221.
- [13] Sheikholeslami, M., Shamlooei, M. and Moradi, R., Fe_3O_4 - Ethylene glycol nanofluid forced convection inside a porous enclosure in existence of Coulomb force, *J. Molec. Liq.* 249 (2018), pp. 429-437.
- [14] 18] Abbas, Z., M, Rafiq and Naveed, M., Analysis of Eyring-Powell liquid flow in curved channel with Cattaneo-Christov heat flux model, *Braz. J. Mech. Sci. Eng.* (2018).
- [15] Sheikholeslami, M. and Rokni, H. B., Numerical simulation for impact of Coulomb force on nanofluid heat transfer in a porous enclosure in presence of thermal radiation, *Int. J. Heat Mass Transf.* 118 (2018), pp. 823-831.
- [16] Sheikholeslami, M. and Sadoughi, M. K., Simulation of CuO - water nanofluid heat transfer enhancement in presence of melting surface, *Int. J. Heat Mass Transf.* 116 (2018), pp. 909-919.
- [17] Makinde, O. A. and Aziz, A., Boundary layer flow of a nanofluid past a stretching sheet with a convective boundary condition, *Int. J. Therm. Sci.* 50 (2011), pp. 1326-1332.
- [18] Naveed, M., Abbas, Z. and Sajid, M., Thermophoresis and Brownian effects on the Blasius flow of a nanofluid due to curved surface with thermal radiation, *Euro. Phy. J. Plus* (2016) 131:214.
- [19] Naveed, M., Abbas, Z. and Sajid, M., Nonlinear radiative heat transfer in Blasius and Sakiadis flows over a curved surface, *Int. J. ThermoPhysics* (2017) 38:14.
- [20] Naveed, M., Abbas, Z. and Sajid, M., Effect of Homogeneous-heterogeneous reactions and magnetohydrodynamics on nanofluid for the Blasius flow with thermal radiation, *J. Molec. Liq.* 233 (2017), pp. 115-121.
- [21] Jafar, K., Nazar, R., Ishak, A., and Pop, I., MHD flow and heat transfer over stretching/shrinking sheet with external magnetic field, viscous dissipation and Joule effects. *Canad. J. Chem. Eng.*, 999 (2011), pp. 1-11.
- [22] Kameswaran, P. K., Narayana, M., Sibanda, P., and Murthy, P. V. S. N., Hydromagnetic nanofluid due to a stretching or shrinking sheet with viscous dissipation and chemical reaction effects, *Int. J. Heat Mass Trans.* 55 (2012), pp. 7587-7595.
- [23] Rosca, A., MHD boundary layer flow over a permeable shrinking surface, *Acta Uni. Apul.* 36 (2013), pp. 31-38.
- [24] Mishra, S. R., and Jena, S., Numerical solution of boundary layer MHD flow with viscous dissipation, *Sci. World J.* 756498 (2014).
- [25] Sheikholeslami, M. and Rokni, H. B., CVFEM for effect of Lorentz forces on nanofluid flow in a porous complex shaped enclosure by means of non-equilibrium model, *J. Molec. Liq.* 254 (2018), pp. 446-462.

- [26] Sheikholeslami, M. and Rokni, H. B., Magnetic nanofluid flow and convective heat transfer in a porous cavity considering Brownian motion effects, *Physics of Fluids*, 30 (1) (2018).
- [27] Sheikholeslami, M., Numerical investigation for CuO-H₂O nanofluid flow in a porous channel with magnetic field using mesoscopic method, *J. Molec. Liq.* 249 (2018), pp. 739-746.
- [28] Sheikholeslami, M., CuO-water nanofluid flow due to magnetic field inside a porous media considering Brownian motion, *J. Molec. Liq.* 249 (2018), pp. 921-929.
- [29] Sheikholeslami, M. and Shehzad, S. A., Numerical analysis of $Fe_3O_4-H_2O$ nanofluid flow in permeable media under the effect of external magnetic source, *Int. J. Heat Mass Transf.* 118 (2018), pp. 182-189.
- [30] Sheikholeslami, M. and Rokni, H. B., Simulation of nanofluid heat transfer in presence of magnetic field: A review, *Int. J. Heat Mass Transf.* 115 (2017), pp. 1203-1233.
- [31] Sheikholeslami, M., Influence of magnetic field on nanofluid free convection in an open porous cavity by means of Lattice Boltzmann method, *J. Molec. Liq.* 234 (2017), pp. 364-374.
- [32] Sajid, M., Ali, N., Javed, T., and Abbas, Z., Stretching a curved surface in a viscous fluid, *Chin. Phy. Lett.* 27 (2010), 024703 .
- [33] Abbas, Z., Naveed, M., and Sajid, M., Heat transfer analysis for stretching flow over curved surface with magnetic field, *J. Eng. Therm.* 22 (2013), pp.337-345.
- [34] Naveed, M., Abbas, Z., and Sajid, M., MHD flow of a micropolar fluid due to a curved stretching sheet with thermal radiation, *J. Appl. Fluid Mech.* 9 (2013), pp. 131-138.
- [35] Abbas, Z., Naveed, M., and Sajid, M., Hydromagnetic slip flow of nanofluid over a curved stretching surface with heat generation and thermal radiation, *J. Mole. Liq.* 215 (2016), pp. 756-762.
- [36] Khan, W. A., and Pop, I., Boundary layer flow of a nanofluid past a stretching sheet, *Int. J. Heat Mass Trans.* 53 (2010), pp. 2477-2483.
- [37] Wang, C. Y., Free convection on a vertical stretching surface, *J. Appl. Math. Mech.* (ZAMM). 69 (1989), pp. 418-420.